Electrophilic Aromatic Coupling of Hexapyrrolylbenzenes. A Mechanistic Analysis

Supplementary Information

by Maksim Navakouski, Halina Zhylitskaya, Piotr J. Chmielewski, Marika Żyła-Karwowska, and Marcin Stępień*

Table of Contents

Experimental 2

Additional Figures 4

Additional Tables 15

NMR Spectra 18

Mass Spectra 23

References 26

Experimental

Computational methods. Density functional theory (DFT) calculations were performed using Gaussian 09.[1] DFT geometry optimizations were carried out in unconstrained C_1 symmetry, using molecular mechanics or semiempirical models as starting geometries. DFT geometries were refined to meet standard convergence criteria, and the existence of a stationary point was verified by a normal mode frequency calculation. Geometry optimizations, frequency calculations, and thermochemistry calculations were performed using the hybrid functional B3LYP[2–4] combined with the 6-31G(d,p) basis set and the GD3BJ dispersion correction.[5] In the calculations of absorption and CD spectra, up to 200 electronic transitions were calculated by means of time-dependent DFT (TD-DFT), using the above level of theory, PCM solvation[6] (standard dichloromethane parameters), and the Tamm–Dancoff approximation (TDA).[7]

Additional Figures

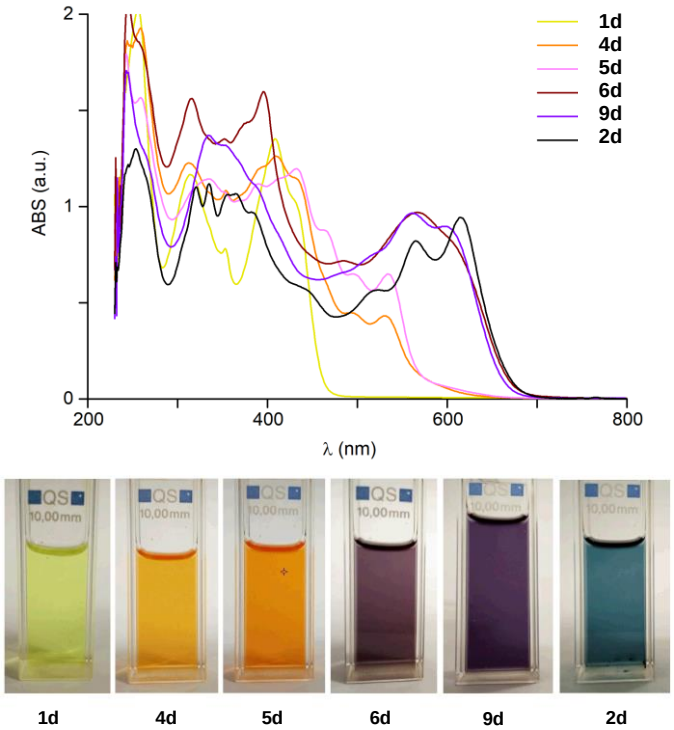

Figure S1. Changes in the optical properties of **1d**, **2d**, and the partially coupled intermediates.

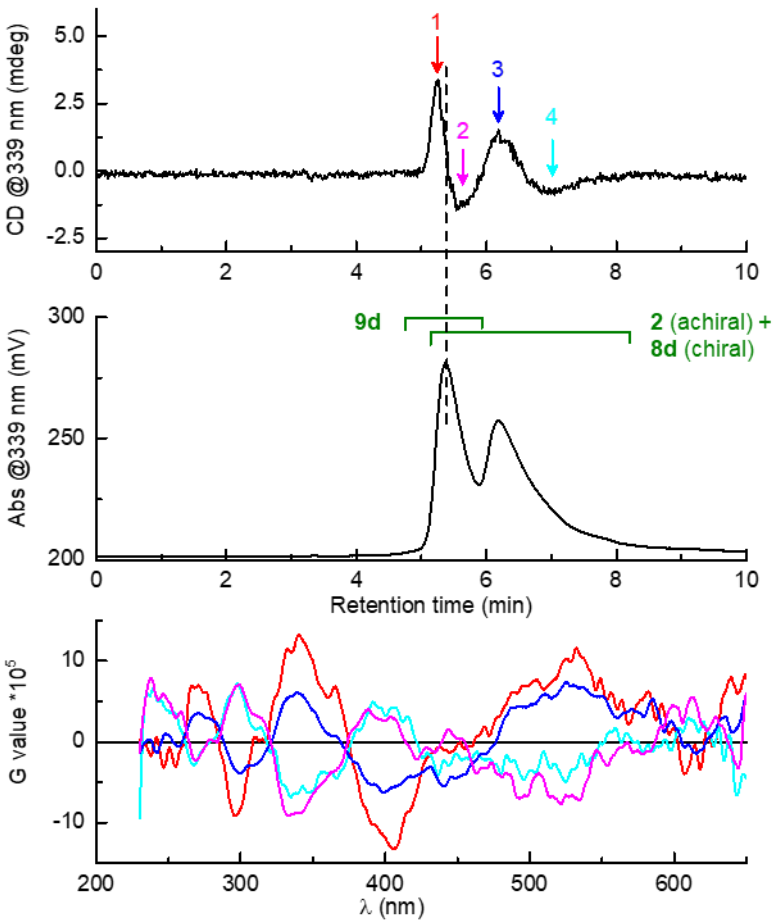

Figure S2. Chiral-phase HPLC chromatograms of a mixture of **8d** and **9d** (Chirex® (S)-Val and (R)-NEA; dichloromethane/*n*-hexane, 80/20; NEA = 1-(α-naphthyl)ethylamine) monitored using CD and absorption spectroscopy (top and center, respectively). CD spectra recorded at specific elution times (points 1–4, red, purple, blue, and cyan, respectively) are shown in the bottom panel. **9d** partly converts to **2d** during the separation. The presence of **9d**, **8d** and **2d** in specific fractions was verified using ^{1}H NMR spectroscopy.

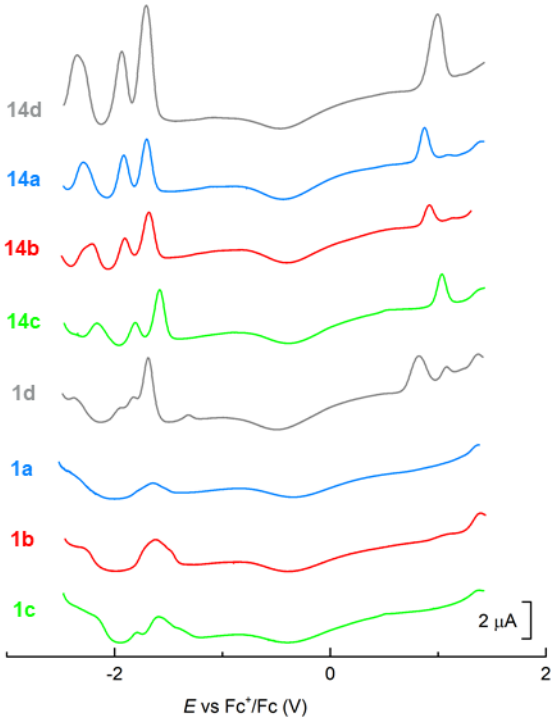

Figure S3. Differential pulse voltammograms for pyrroles **14a**-**d** and hexapyrrolylbenzenes **1a**-**d**.

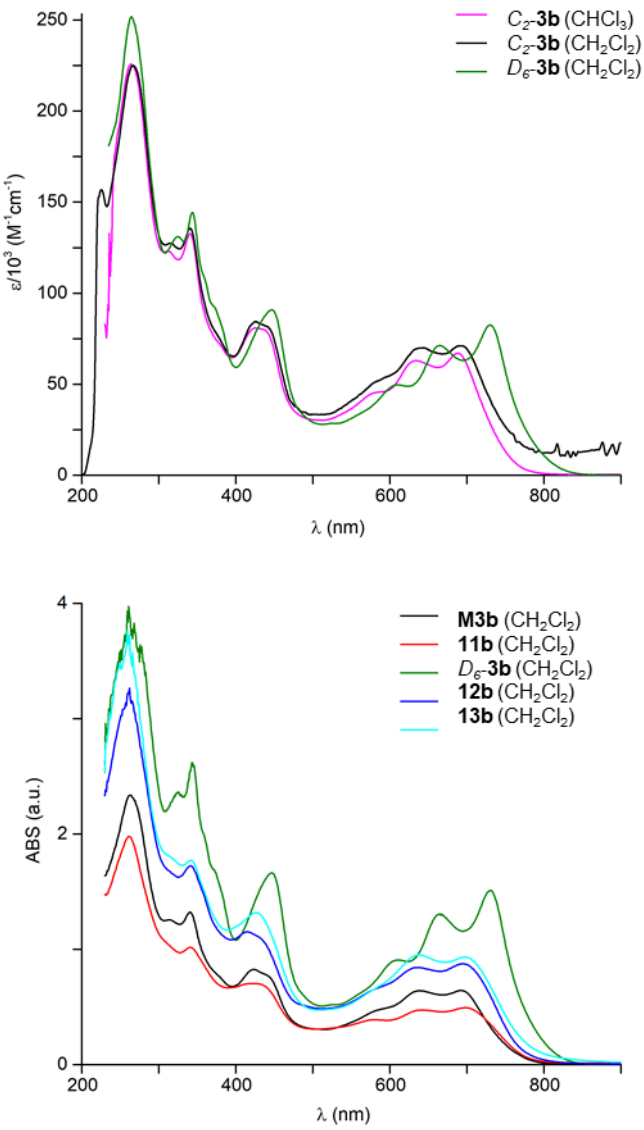

Figure S4. Top: Electronic spectra of C_2-**3b** and D_6-**3b**. Bottom: Comparison of absorption spectra for the **11b**–**13b** and **M3b** byproducts isolated in the reaction of **1b** with *N*-bromosuccinimide in dioxane (cf. general procedures for the synthesis of hexapyrrolohexaazacoronenes, Variant 2). See also Scheme 2 for proposed structures of these byproducts. **M3b** is an inseparable mixture of C_2-**4b** and the additional low-symmetry isomers of **4b**. The blue-shifted absorptions of **11b**, **12b**, and **13b**, in comparison with D_6-**3b**, are consistent with the proposed incomplete fusion of the HPHAC core.

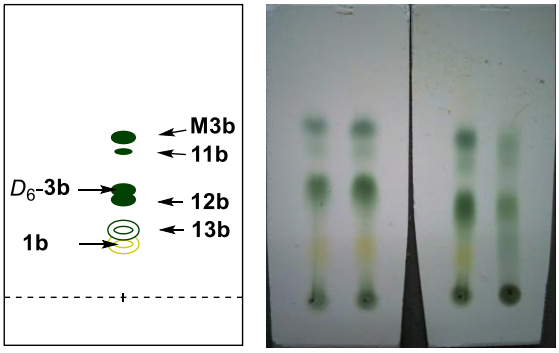

Figure S5. Thin layer chromatograms (alumina, toluene/ethyl acetate = 10/1, v/v) obtained for crude mixtures from reaction of **1b** with *N*-bromosuccinimide in dioxane without addition of acid (Scheme 2). **M3b** is an inseparable mixture of C_2-**3b** and the additional low-symmetry isomers of **3b**.

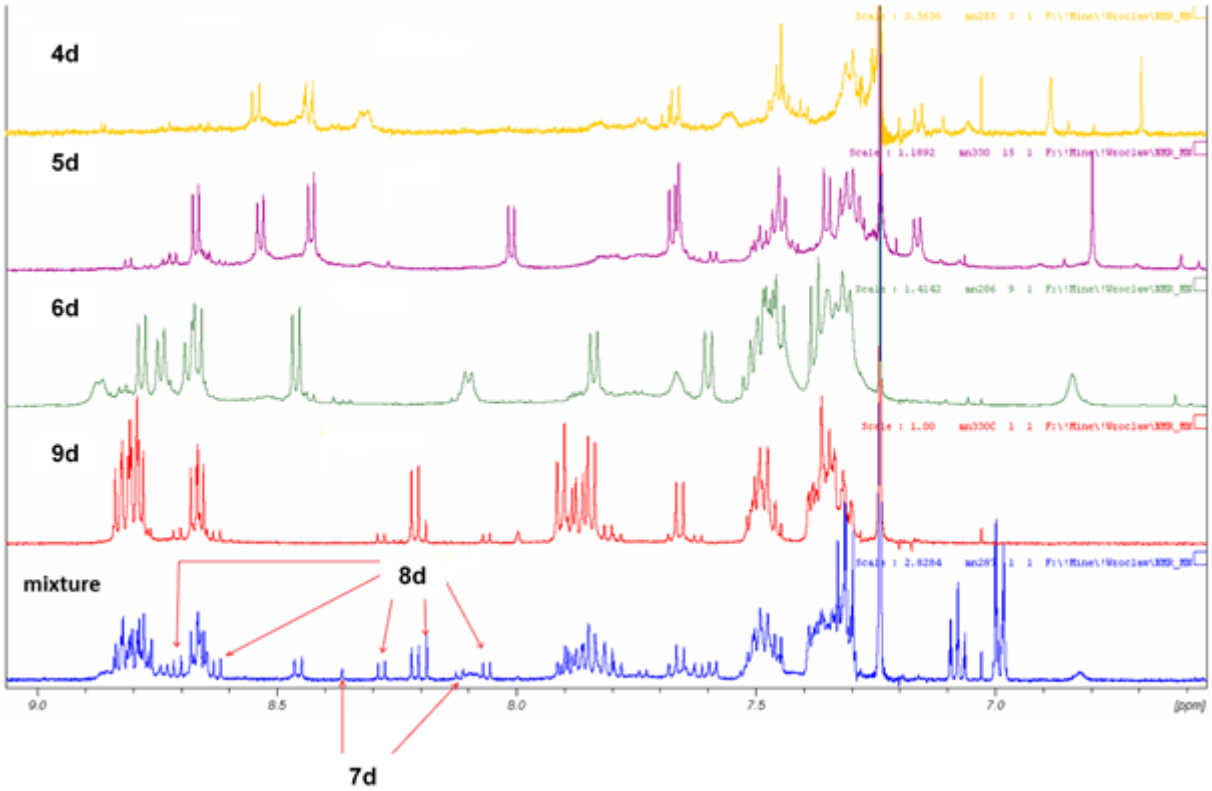

Figure S6. ^{1}H NMR spectra of a crude mixture of coupling products, containing **6d**–**19d** (blue trace), and partly separated **4d**, **5d**, **6d**, and **9d** (chloroform-*d*).

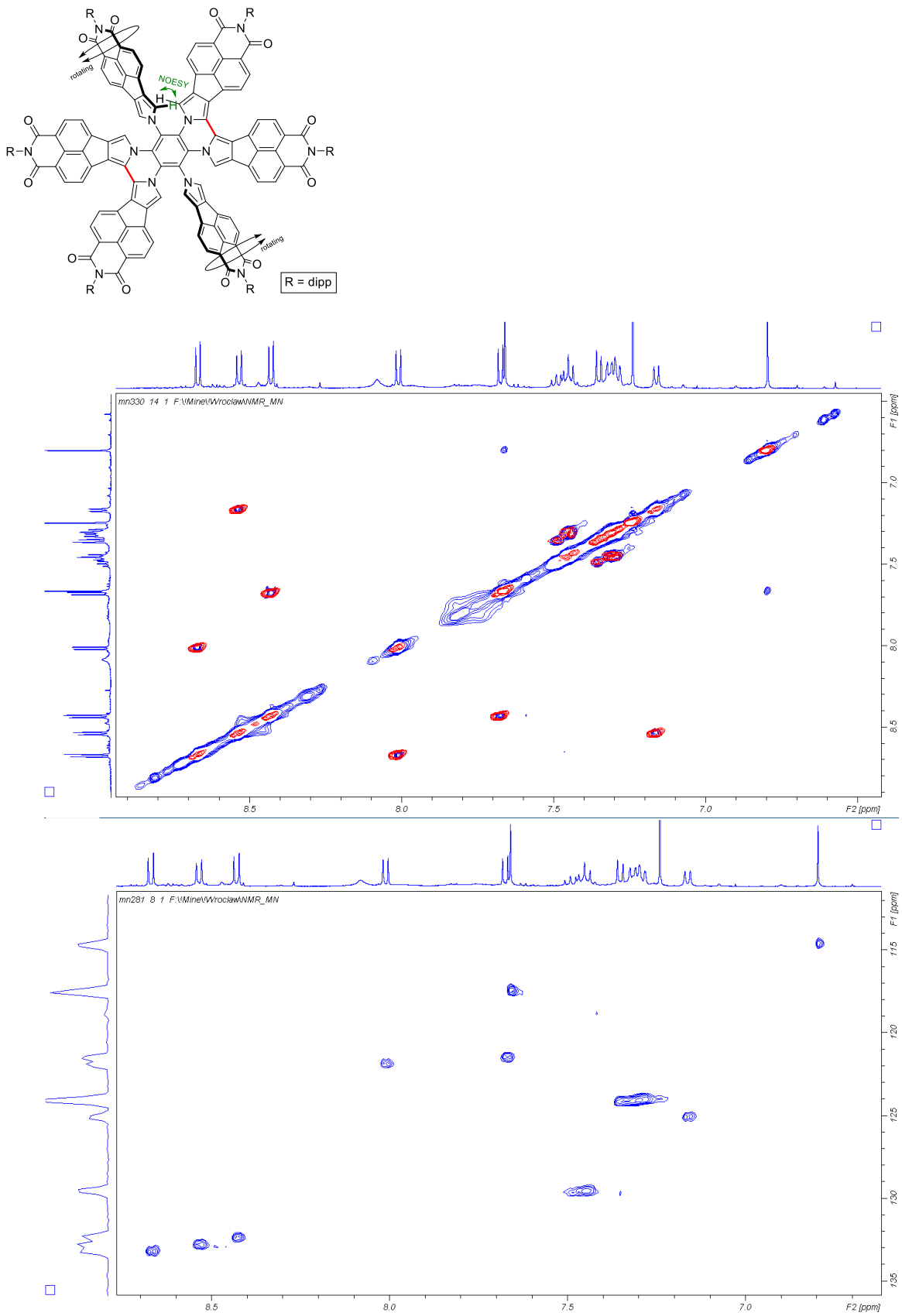

Figure S7. 2D NMR correlation spectra recorded for **5d**. Top: structure with the key NOESY correlation (green arrow); center: overlaid COSY (red) and NOESY (blue); bottom: HSQC spectrum of the aromatic region.

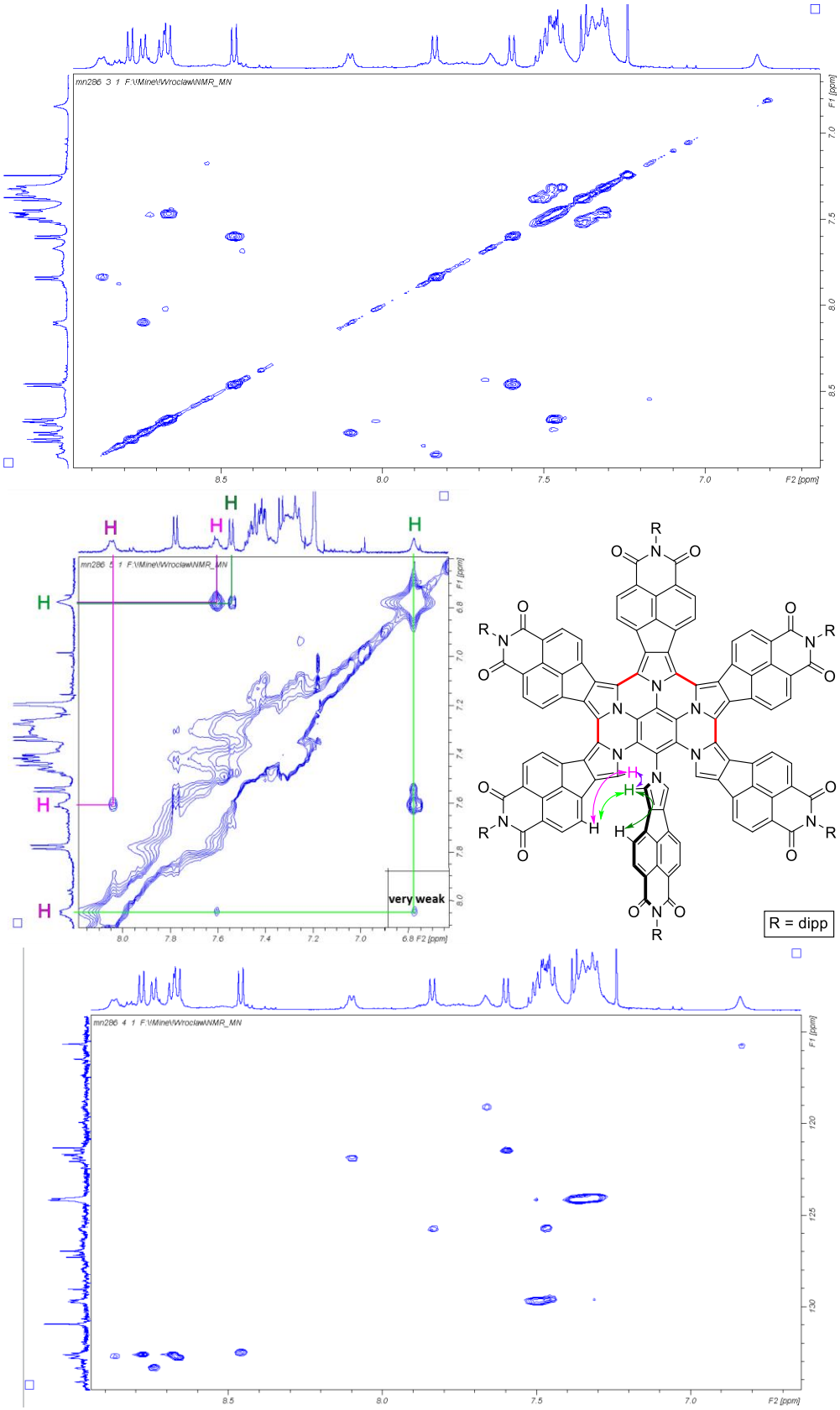

Figure S8. 2D NMR correlation spectra recorded for **6d**: top – COSY, center – NOESY with lines showing correlations involving alpha-protons ; bottom – HSQC.

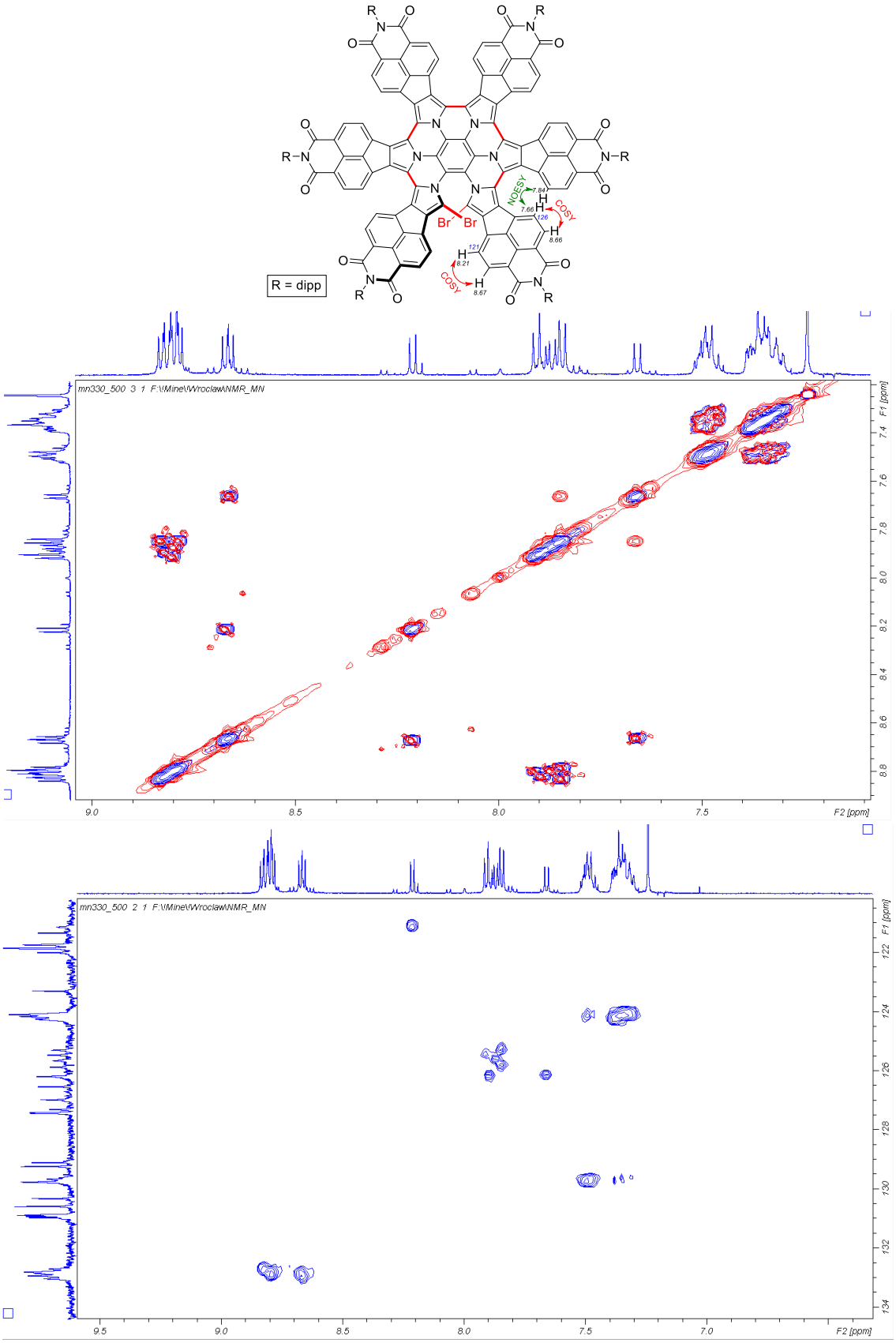

Figure S9. 2D NMR correlation spectra recorded for **9d**. Top: structure with NOESY correlations (green arrow); center: overlaid COSY (blue) , and NOESY (red); bottom: HSQC. In the sample there is an admixture of **2d**.

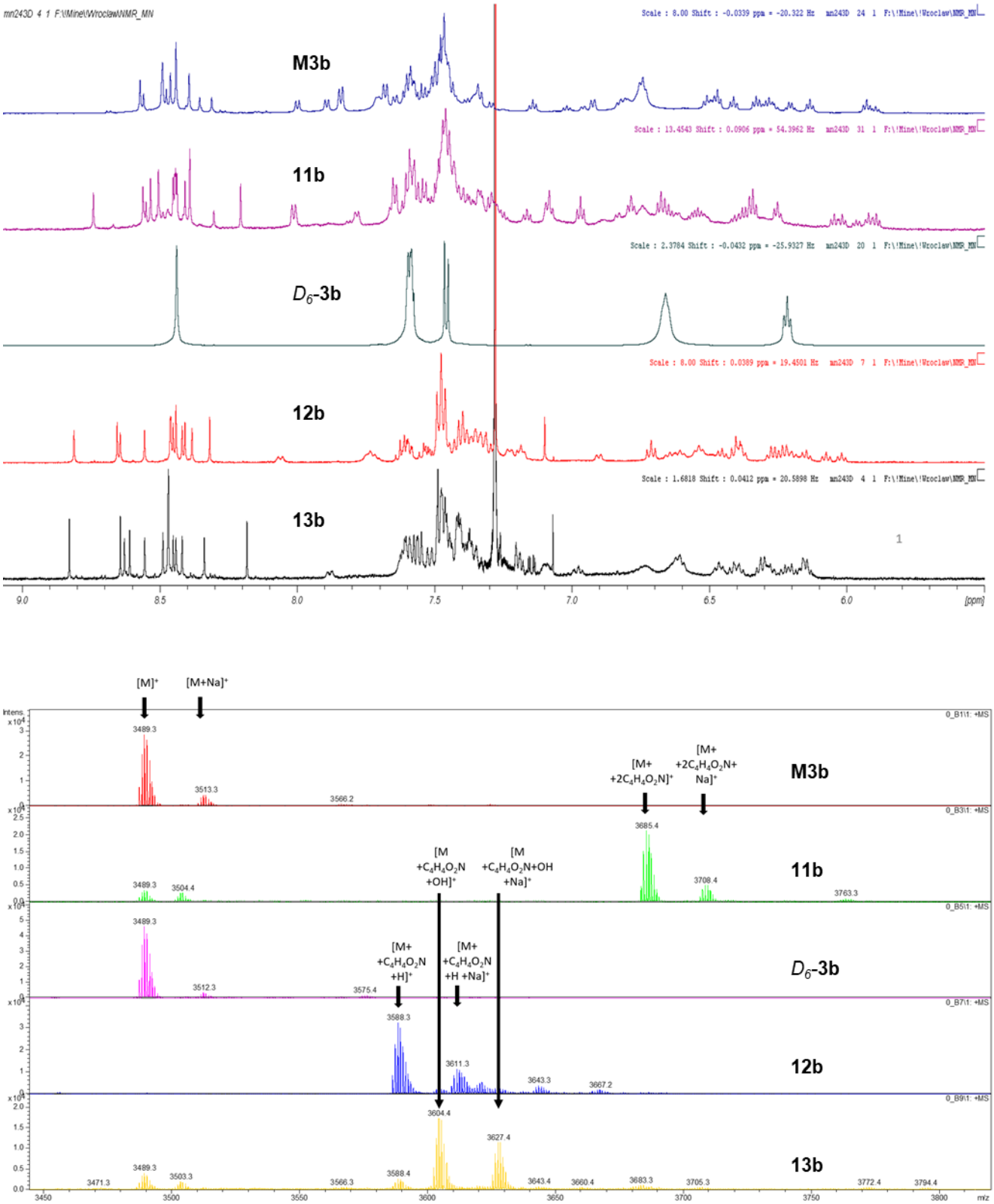

Figure S10. ^{1}H-NMR (chloroform-*d*; *top*) and MALDI-TOF (*bottom*) spectra of the major byproducts formed in the reaction of **1b** with *N*-bromosuccinimide in dioxane.

Additional Tables

Table S1. Redox potentials (in volts vs. ferrocene internal standard) from differential pulse voltammetry of dichloromethane solutions with tetrabutylammonium hexafluorophosphate as a supporting electrolyte, glassy carbon working electrode, platinum wire counter electrode, and silver chloride reference electrode.

Compound	E_{red1}	E_{red2}	E_{red3}	E_{red4}	E_{red5}	E_{red6}	E_{red7}	E_{red8}	E_{ox1}	E_{ox2}	E_{ox3}	E_{ox4}	HLG
D_6-**3a**	–1.36	–1.46	–1.59	–1.72	–1.84	–1.97	–2.27	–2.40	0.15	0.29	1.00	1.11	1.51
D_6-**3b**	–1.35	–1.45	–1.57	–1.70	–1.83	–1.95	–2.24	–2.36	0.16	0.32	1.01		1.51
C_2-**3b**	–1.36	–1.47	–1.58	–1.68	–1.78	–1.89	–2.15	–2.29	0.22	0.39	1.09		1.58
D_6-**3c**	–1.22	–1.34	–1.50	–1.66	–1.79	–2.08	–2.21	–2.40	0.37	0.68			1.59
1d	–1.69	–1.83	–1.95	–2.38					0.82[b] (0.52, 0.65)[c]	1.08[b]			2.51
1a	–1.53	–1.64	–1.79						no well-defined oxidation				
1b	–1.48	–1.62	–1.70	–2.30					no well-defined oxidation				
1c	–1.38	–1.59	–1.79	–2.14					no well-defined oxidation				
14d	–1.71	-1.93[b]	–2.29	–2.35					1.00				2.70
14a	–1.70	-1.91[b]	–2.29						0.87[b]				2.58
14b	–1.68	–1.90	–2.21	–2.27					0.92[b]	1.14			2.60
14c	–1.58	-1.81[b]	–2.17						1.04[b]				2.62

[a] Irreversible couple. [b] Partially reversible couple. [c] Products of irreversible oxidation.

Table S2. Computational data.

Code[a]	Mult[b]	SCF E[c,d] a.u.	ZPV[c,e] a.u.	lowest freq.[c,f] cm^{-1}	*G*[c,g] a.u.	$<S^2>$[h]
9d'_bsS	1	–10609.000019	1.086362	8.93	–10608.036555	0.00
9d'_T	3	–10608.940888	1.081232	8.22	–10607.984099	2.00
9d'_TS_bsS	1	–10608.959551	1.083369	–593.77	–10607.998457	0.00
9d'_TS_T	3	–10608.926731	1.081983	–128.64	–10607.968477	2.00
2d'.2Br_bsS	1	–10608.988563	1.086328	6.20	–10608.027911	0.12
2d'.2Br_T	3	–10608.989496	1.086208	6.31	–10608.029793	2.00
Br2	1	–5143.401907	0.000746	327.59	–5143.425311	0.00

[a] Structure code (see the zip file for Cartesian coordinates). [b] Multiplicity. [c] GD3BJ-B3LYP/6-31G(d,p) energies and geometries. [d] SCF electronic energy. [e] Zero-point vibrational energy. [f] lowest vibrational frequency. [g] Gibbs free energy. [h] After annihilation of the first spin contaminant.

NMR Spectra

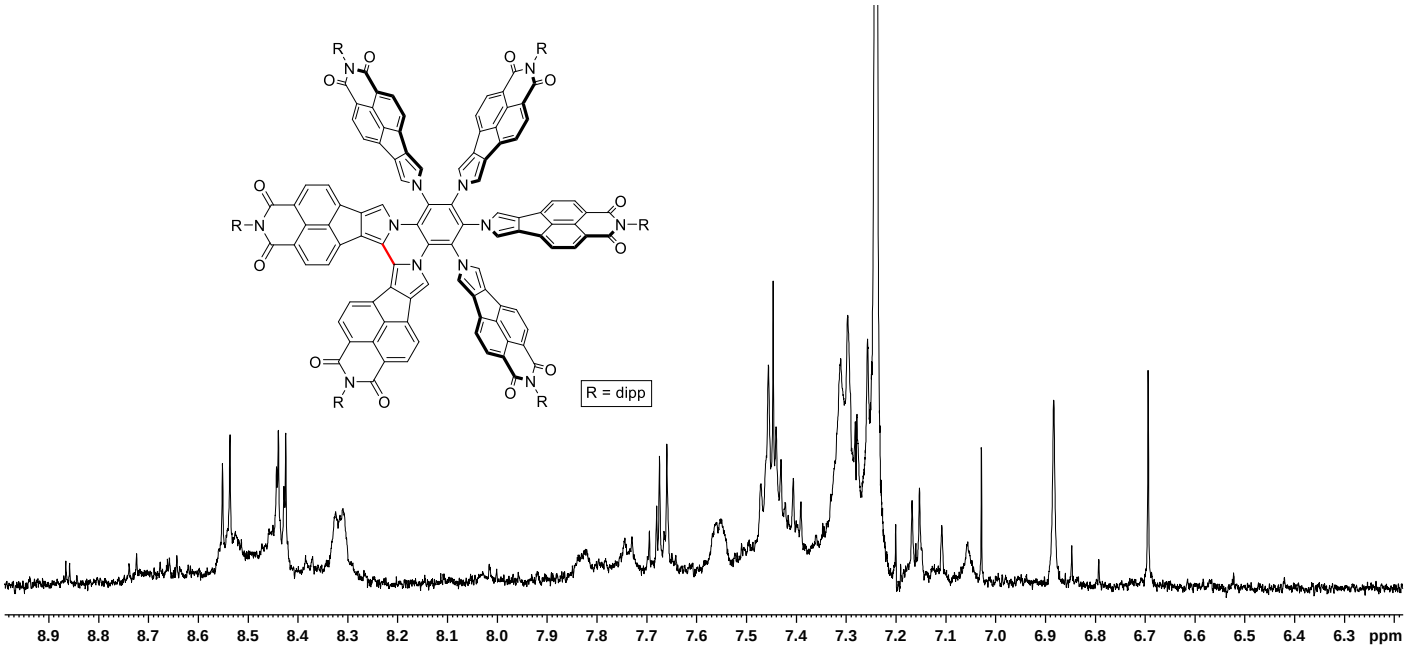

Figure S11. ^{1}H NMR spectrum of crude **4d** (500 MHz, chloroform-*d*, 300 K).

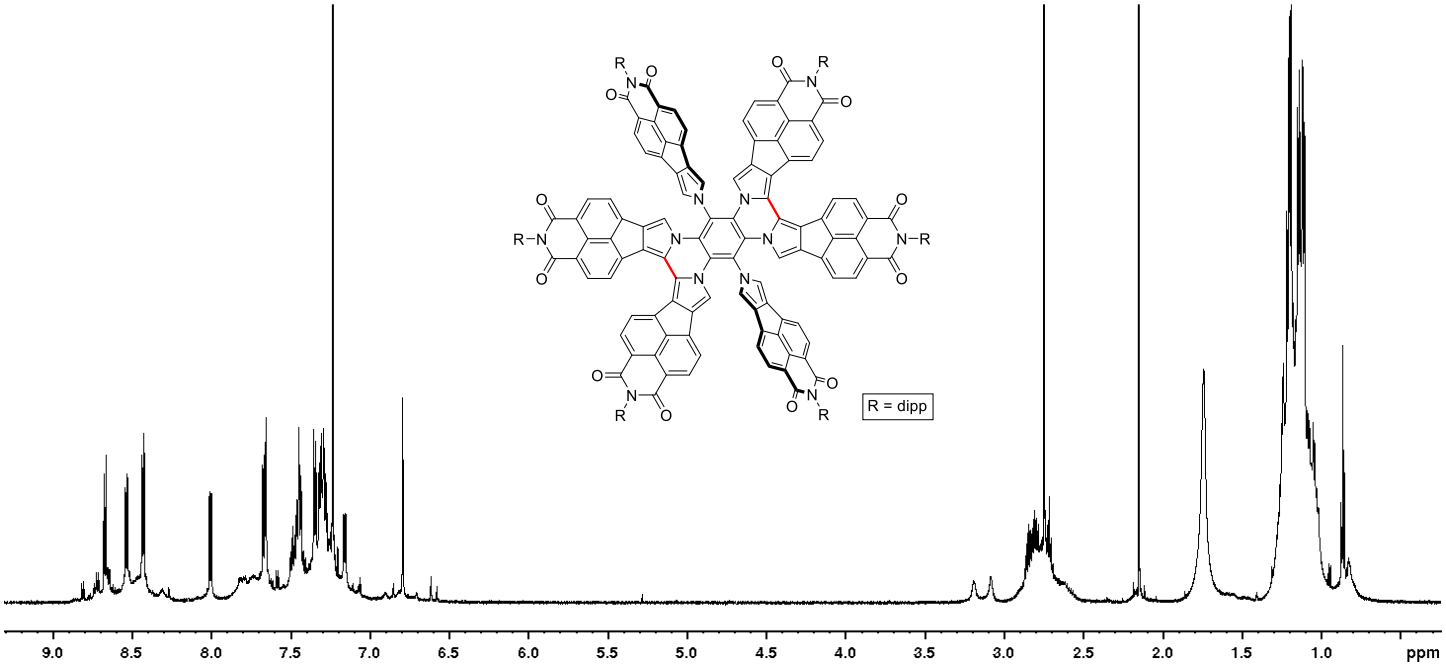

Figure S12. ^{1}H NMR spectrum of crude **5d** (600 MHz, chloroform-*d*, 300 K).

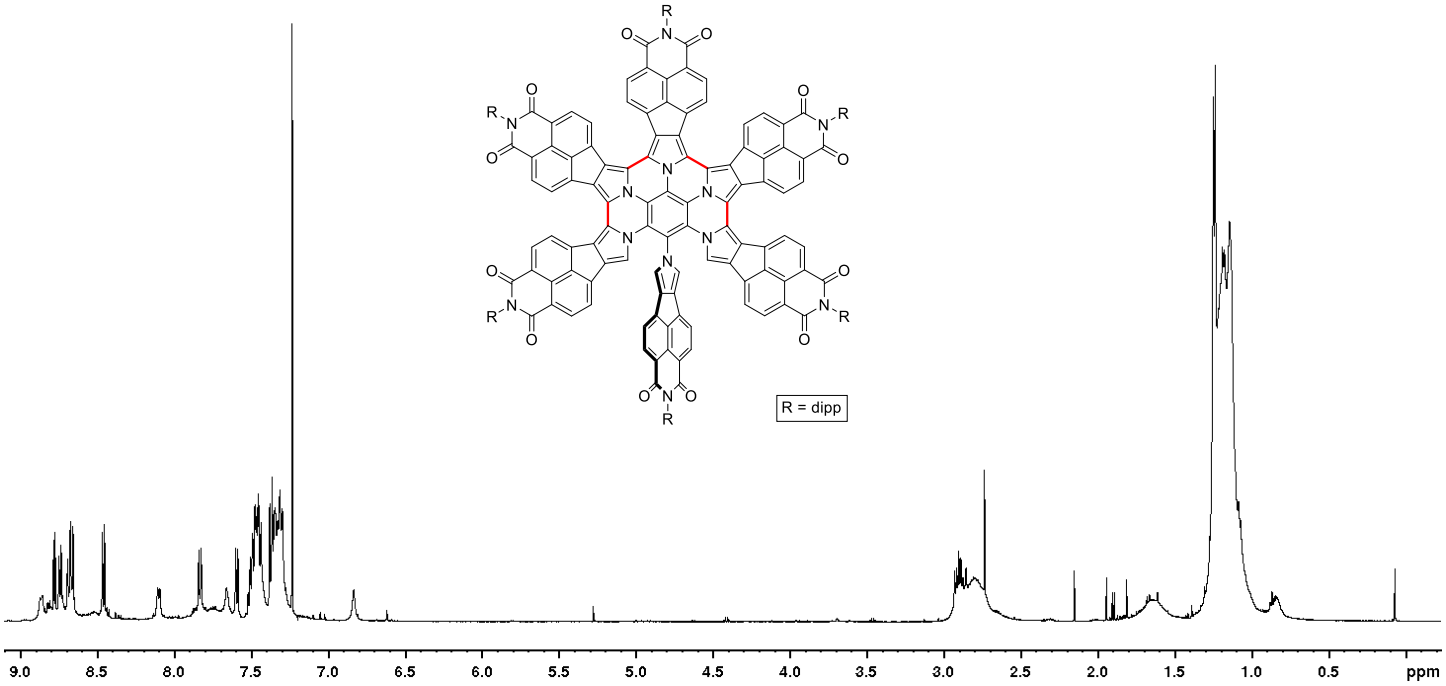

Figure S13. ^{1}H NMR spectrum of crude **6d** (500 MHz, chloroform-*d*, 300 K).

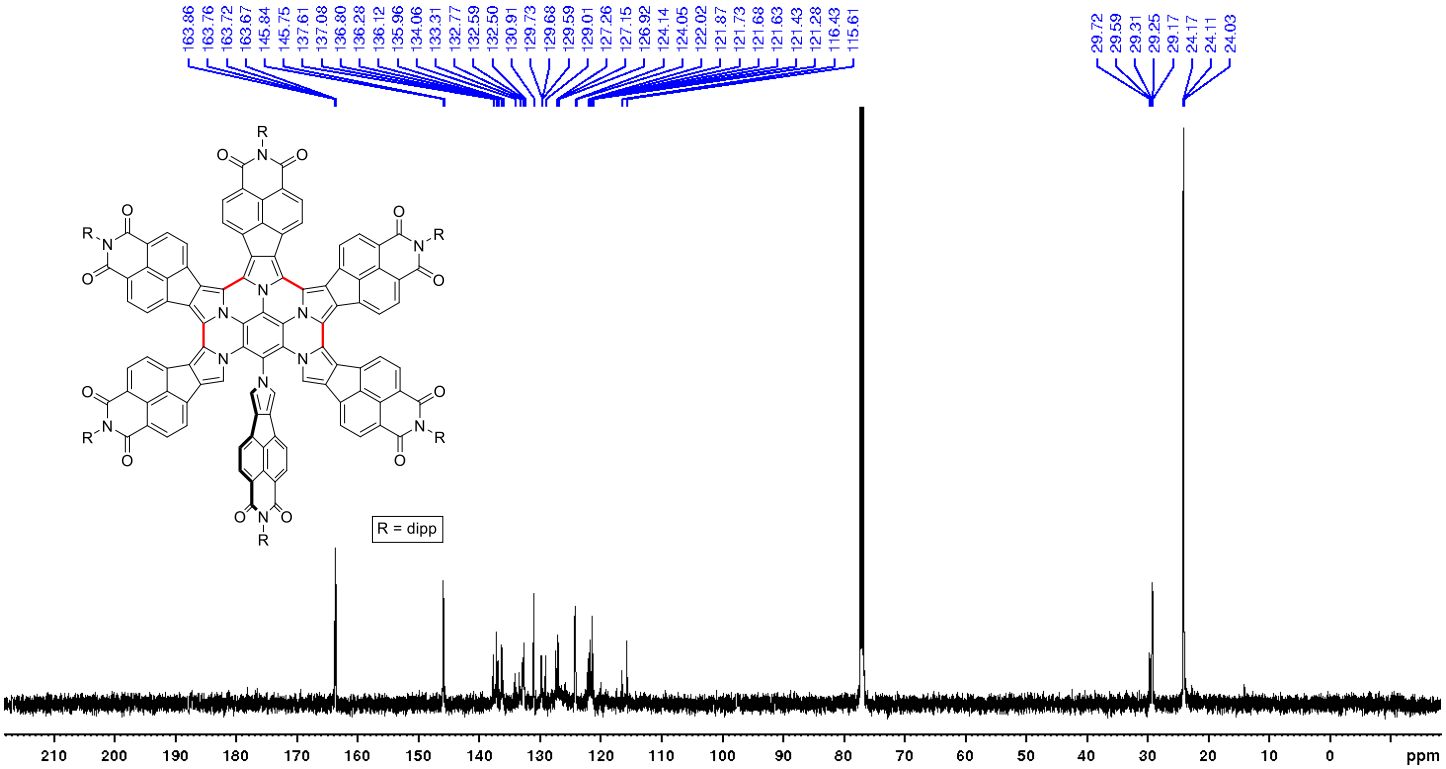

Figure S14. ^{13}C NMR spectrum of crude **6d** (125 MHz, chloroform-*d*, 300 K).

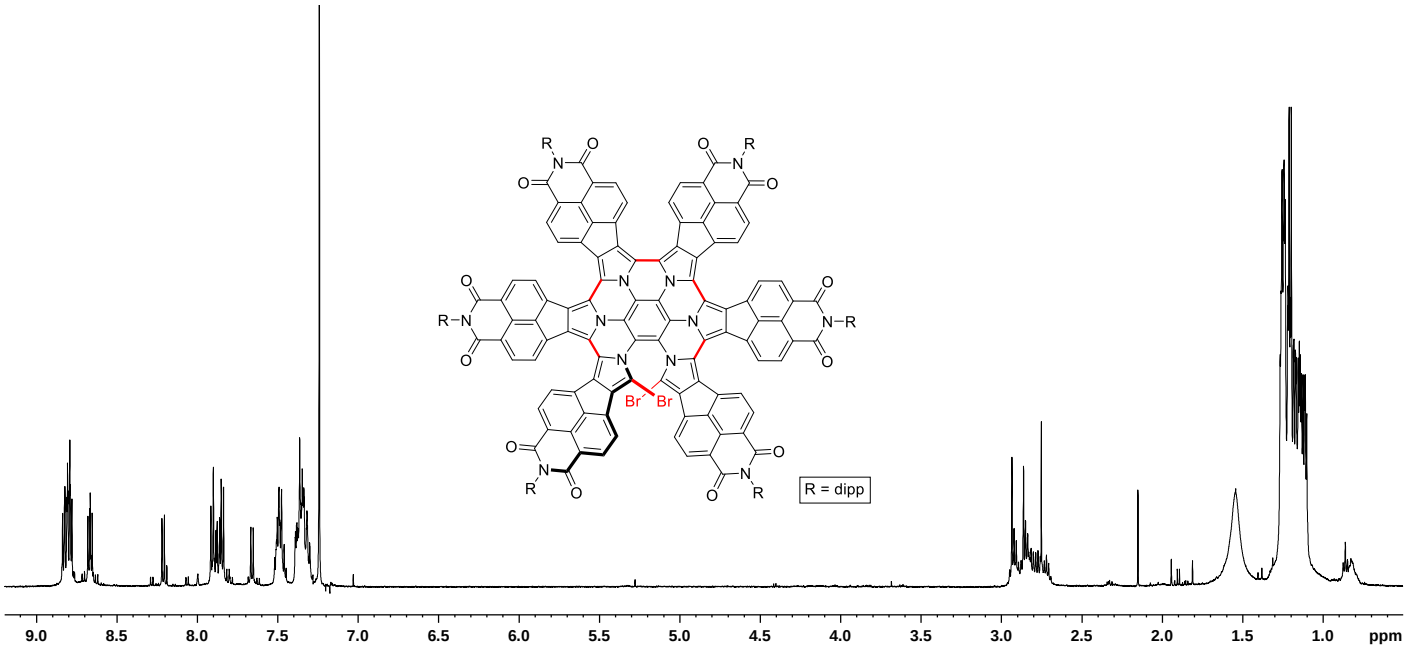

Figure S15. ^{1}H NMR spectrum of **9d** (500 MHz, chloroform-*d*, 300 K).

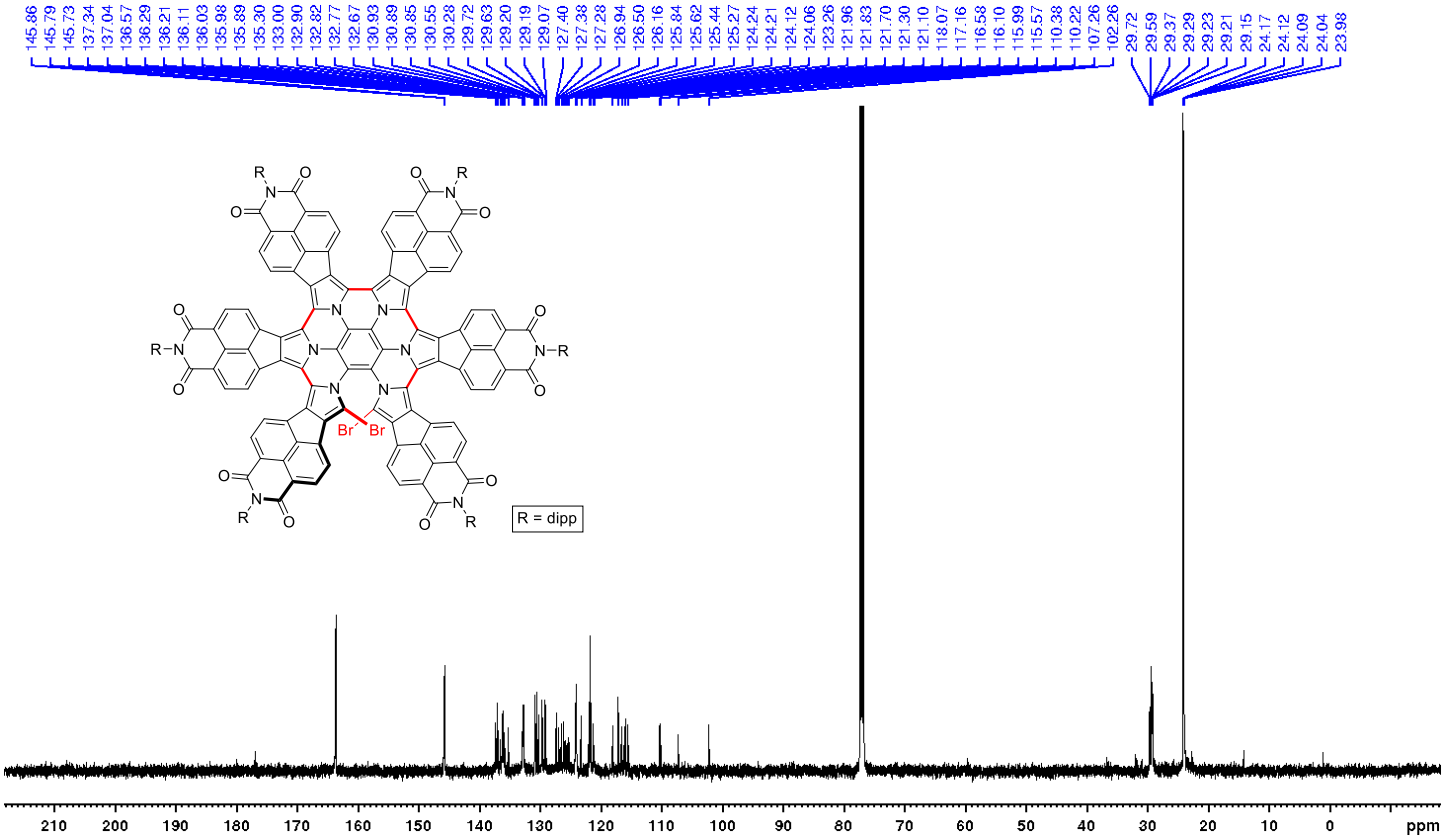

Figure S16. ^{13}C NMR spectrum of **9d** (125 MHz, chloroform-*d*, 300 K).

Mass Spectra

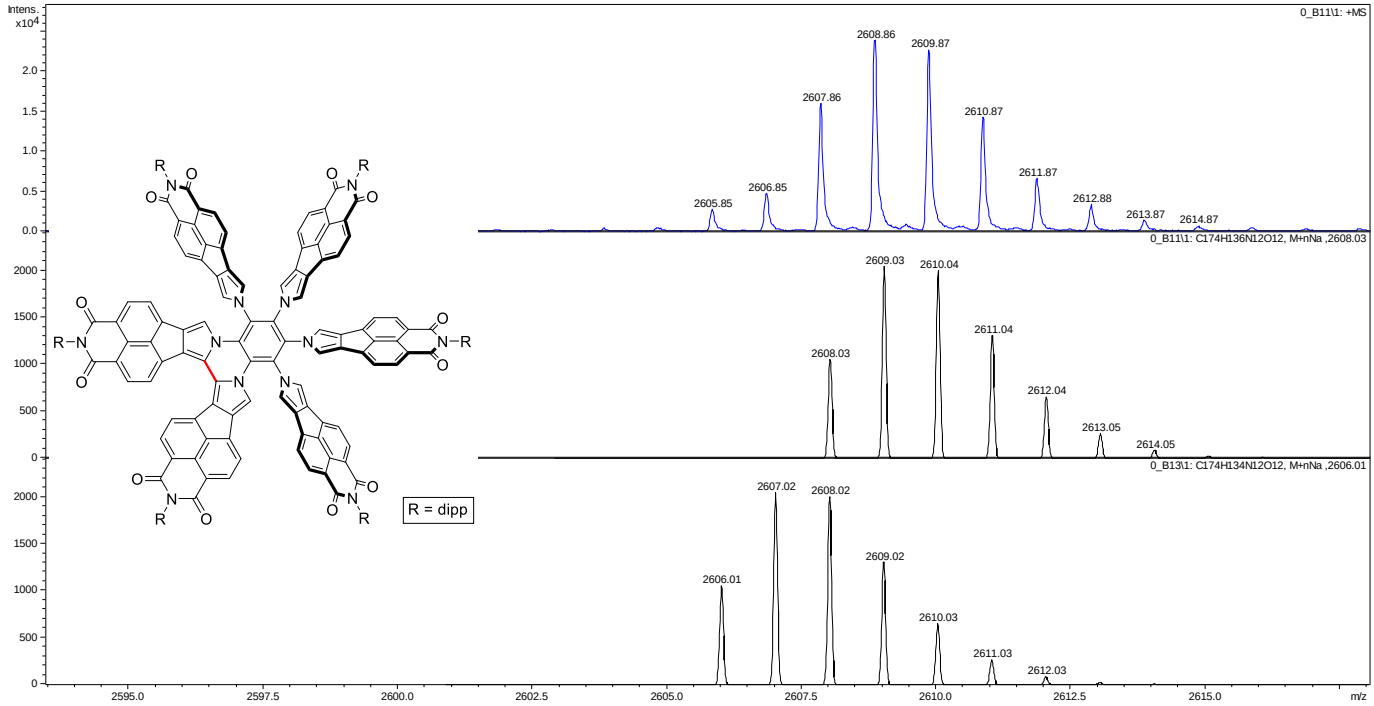

Figure S17. Mass spectrum of **4d** (MALDI–TOF, top: experimental, middle: simulated, bottom: simulated).

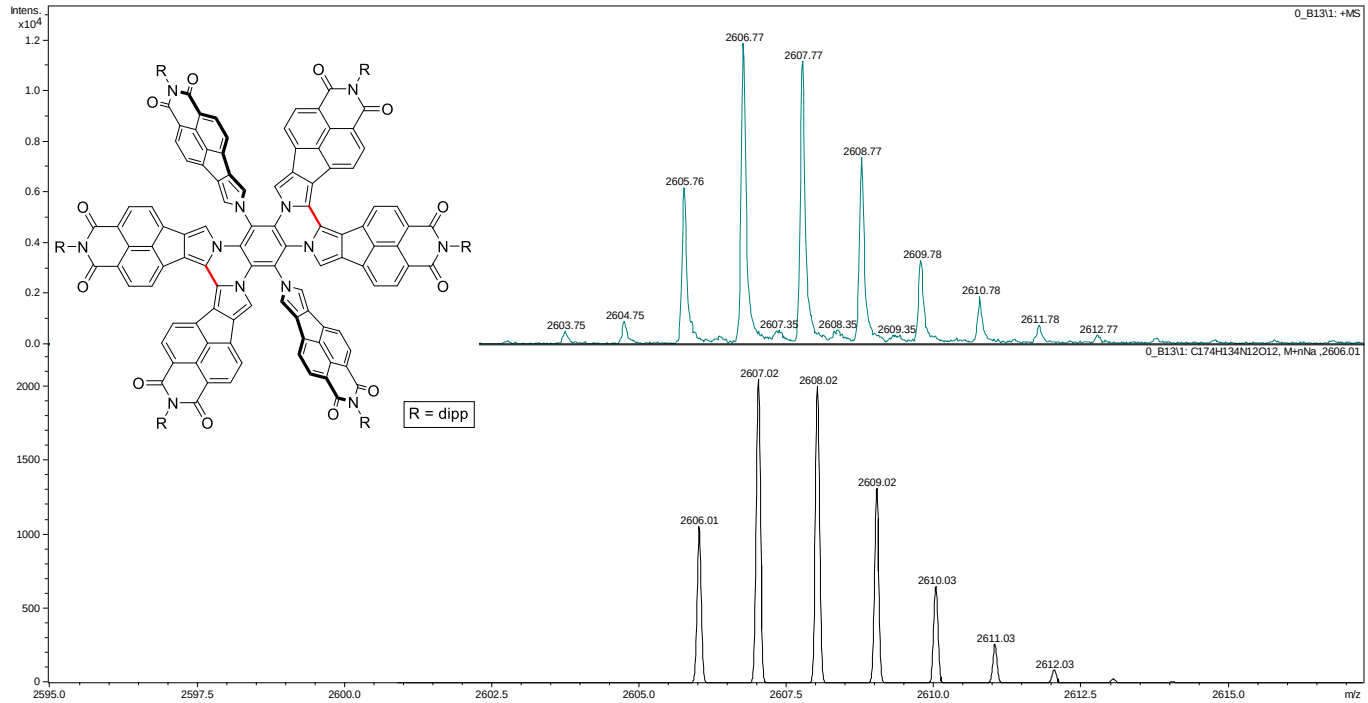

Figure S18. Mass spectrum of **5d** (MALDI–TOF, top: experimental, bottom: simulated).

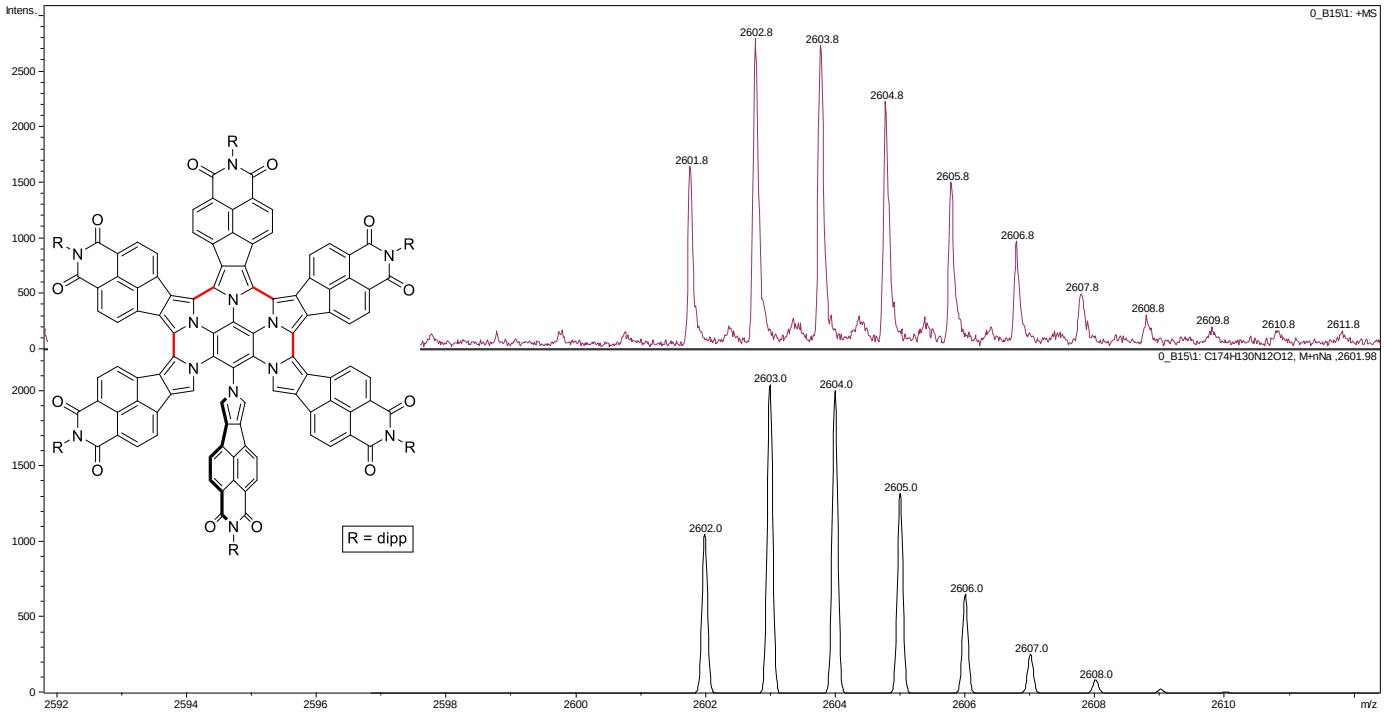

Figure S19. Mass spectrum of **6d** (MALDI–TOF, top: experimental, bottom: simulated).

References

(1) Frisch, M. J.; Trucks, G. W.; Schlegel, H. B.; Scuseria, G. E.; Robb, M. A.; Cheeseman, J. R.; Scalmani, G.; Barone, V.; Mennucci, B.; Petersson, G. A.; et al. *Gaussian 09 Revision E.01*; Gaussian Inc.: Wallingford CT, 2009.
(2) Becke, A. D. Density-Functional Exchange-Energy Approximation with Correct Asymptotic Behavior. *Phys. Rev. A* **1988**, *38* (6), 3098–3100.
(3) Becke, A. D. Density-functional Thermochemistry. III. The Role of Exact Exchange. *J. Chem. Phys.* **1993**, *98* (7), 5648–5652. https://doi.org/10.1063/1.464913.
(4) Lee, C.; Yang, W.; Parr, R. G. Development of the Colle-Salvetti Correlation-Energy Formula into a Functional of the Electron Density. *Phys. Rev. B* **1988**, *37* (2), 785–789. https://doi.org/10.1103/PhysRevB.37.785.
(5) Grimme, S.; Ehrlich, S.; Goerigk, L. Effect of the Damping Function in Dispersion Corrected Density Functional Theory. *J. Comput. Chem.* **2011**, *32* (7), 1456–1465. https://doi.org/10.1002/jcc.21759.
(6) Tomasi, J.; Mennucci, B.; Cammi, R. Quantum Mechanical Continuum Solvation Models. *Chem. Rev.* **2005**, *105* (8), 2999–3094. https://doi.org/10.1021/cr9904009.
(7) Hirata, S.; Head-Gordon, M. Time-Dependent Density Functional Theory within the Tamm–Dancoff Approximation. *Chem. Phys. Lett.* **1999**, *314* (3–4), 291–299. https://doi.org/10.1016/S0009-2614(99)01149-5.
(8) Navakouski, M.; Zhylitskaya, H.; Chmielewski, P. J.; Lis, T.; Cybińska, J.; Stępień, M. Stereocontrolled Synthesis of Chiral Heteroaromatic Propellers with Small Optical Bandgaps. *Angew. Chem. Int. Ed.* **2019**, *58* (15), 4929–4933. https://doi.org/10.1002/anie.201900175.
(9) Zhylitskaya, H.; Cybińska, J.; Chmielewski, P.; Lis, T.; Stępień, M. Bandgap Engineering in π-Extended Pyrroles. A Modular Approach to Electron-Deficient Chromophores with Multi-Redox Activity. *J. Am. Chem. Soc.* **2016**, *138* (35), 11390–11398. https://doi.org/10.1021/jacs.6b07826.